Catalysis Today 144 (2009) 75–80

Contents lists available at ScienceDirect

Catalysis Today

journal homepage: www.elsevier.com/locate/cattod

Efficient production of hydrogen by photo-induced reforming of glycerol at ambient conditions

Vasileia M. Daskalaki, Dimitris I. Kondarides *

Department of Chemical Engineering, University of Patras, GR-26504 Patras, Greece

ARTICLE INFO

Article history:
Available online 30 December 2008

Keywords:
Hydrogen production
Photocatalysis
Reforming
Glycerol
Titanium dioxide
Platinum

ABSTRACT

Photocatalytic reforming of aqueous solutions of glycerol at ambient conditions has been investigated with the use of Pt/TiO_2 photocatalysts and a solar light-simulating source. The effects of platinum loading, photocatalyst content in suspension, glycerol concentration, solution pH and temperature on the reaction rate have been studied in detail. Results obtained show that the reaction proceeds with intermediate production of methanol and acetic acid and eventually results in complete conversion of glycerol to H_2 and CO_2. Optimal results are obtained for TiO_2 photocatalyst loaded with 0.1–0.5 wt.% Pt, whereas further increase of platinum content has a detrimental effect on photocatalytic performance. The reaction is favored over neutral and basic solutions, compared to acidic solutions, and the reaction rate increases substantially with increasing temperature from 40 to 60–80 °C. For high glycerol concentrations (~1 mol L^{-1}) the rate of hydrogen evolution is about two orders of magnitude higher, compared to that obtained for pure water, rendering the process suitable for application. It is concluded that glycerol photoreforming at ambient conditions may provide an efficient and low cost method for the production of renewable hydrogen.

1. Introduction

In recent years there have been intensive efforts toward the development of novel technologies for the production of hydrogen from renewable resources, mainly water and biomass [1]. Among the various biomass-derived compounds proposed as feedstock for hydrogen production, glycerol ($C_3H_8O_3$) is of special interest because it is produced in large amounts (10 wt.%) as by-product of the chemical reaction (transesterification) in which vegetable oil is processed into biodiesel [2]. The world demand for glycerol is limited and in response to the rapid increase in global biodiesel production, crude glycerol is rapidly becoming a waste product with an attached disposal cost. Thus, a growing body of research is currently focusing on developing new technologies and product families to take advantage of a substance that is abundant and cheap. One promising possibility is to use glycerol as a renewable source of hydrogen, which is often defined as the future energy vector. This can be done with the use of several methods including glycerol reforming in the liquid phase [3,4].

In our recent studies, it was shown that hydrogen can be produced in an efficient manner over irradiated Pt/TiO_2 catalysts by photo-induced reforming of a variety of organic compounds, including organic pollutants and biomass-derived components and derivatives [5–7]. This is achieved by combining photocatalytic splitting of water and light-induced oxidation of organic substrates into a single process, which takes place at ambient conditions in the absence of gas-phase oxygen.

In the present study, we investigate photoreforming of glycerol (Eq. (1)) with the use of a solar light simulating source and Pt/TiO_2 photocatalyst.

$$C_3H_8O_3 + 3H_2O \xrightarrow[Pt/TiO_2]{h\nu \geq E_{bg}} 3CO_2 + 7H_2 \quad (1)$$

The effects of several parameters on the rate of hydrogen production are studied, including platinum loading, photocatalyst content in suspension, glycerol concentration, solution pH and temperature.

2. Experimental

Platinized photocatalysts of variable metal loading (0.05–5 wt.% Pt), denoted in the following as x%Pt/TiO_2, were prepared employing the wet impregnation method [8] with the use of TiO_2 powder (Degussa P25) and $(NH_3)_2Pt(NO_2)_2$ (Alfa) as the metal

* Corresponding author at: Department of Chemical Engineering, University of Patras, 1 Karatheodory St., Rion University Campus, GR-26504 Patras, Greece. Tel.: +30 2610 969527; fax: +30 2610 991527.
E-mail address: dimi@chemeng.upatras.gr (D.I. Kondarides).

0920-5861/$ – see front matter © 2008 Elsevier B.V. All rights reserved.
doi:10.1016/j.cattod.2008.11.009

precursor salt. The impregnated support was dried at 110 °C for 24 h, ground, sieved and finally reduced at 300 °C in H_2 flow for 2 h. The nominal platinum loading of catalysts thus prepared, calculated from the amount of metal precursor salt used in each case, was 0.0, 0.05, 0.10, 0.5, 1.0, 2.0, and 5 wt.%. Catalysts were characterized with respect to their specific surface area and phase composition employing nitrogen physisorption at the temperature of liquid nitrogen (BET method) and X-ray diffraction (XRD), respectively. Platinum dispersion and mean crystallite size were estimated with the use of selective chemisorption of H_2 at 25 °C. Details on the apparatus and methods used for catalyst preparation and characterization can be found elsewhere [8].

The apparatus used for photocatalytic experiments consists of a solar light-simulating source, a quartz photoreactor and an on-line analysis system. The lamp housing (Oriel) is furnished with a Xe-arc lamp (Osram XBO 450 W), a set of lenses for light collection and focusing, and a water filter, which serves for the elimination of infrared radiation. The photoreactor is of cubic shape and its top cover has provisions for measurements of solution pH and temperature, as well as connections for inlet/outlet of the carrier gas (Argon). The gas outlet is equipped with a water-cooled condenser which does not allow vapors to escape from the reactor. The analysis system consists of a gas chromatograph (Varian 3800), equipped with a molecular sieve 5A column and a TCD detector, and a CO_2 analyzer (Binos) connected on-line to the exit of the photo-reactor. The carrier gas is high purity Ar (99.999%). The GC is interfaced to a personal computer which enables automatic sampling of the reactor effluent at pre-selected time intervals via an electrically actuated gas sampling valve. The photon flow entering the reactor, measured by chemical actinometry [5], was found to be 3.79×10^{-7} Einstein s^{-1}.

In a typical experiment, a known amount of photocatalyst (usually 80 mg) in powder form ($d < 90$ μm) is dispersed in triply distilled water (60 mL) under continuous stirring, followed by addition of glycerol. When desired, the solution pH is adjusted with the use of NaOH or HNO_3. The top cover is then put in place and the cell is purged with flowing Ar to remove atmospheric oxygen from the reactor and tubing. The reactor is heated to the desired temperature (40 °C, unless otherwise indicated) and then exposed to light (at $t = 0$) under continuous stirring. Experiments were conducted under an Ar flow of 20 cm^3 min^{-1}, which serves as means of collection and transfer of gaseous products to the analysis system.

Analysis of compounds in solution has been achieved with the use of HPLC and GC. Glycerol concentration was measured on a liquid chromatograph (Waters 501) equipped with a Supelcogel-H column and a reflective index detector (RID-10A, Shimadzu), with the use of a 0.1% H_3PO_4 solution as eluent. For the quantification of acids and alcohols, 1 mL of sample acidified with 30 μL of 20% H_2SO_4 was analyzed on a gas chromatograph (Varian CP-30), equipped with an HP-FFAP column (Agilent Technologies) and a flame ionization detector.

3. Results and discussion

3.1. Catalyst characterization

Results of BET and XRD measurements showed that the synthesized x%Pt/TiO_2 catalysts have, practically, the same specific surface area (40–44 m^2 g^{-1}) and anatase content (ca. 75%). Metal dispersion (D%) of samples containing 0.05, 0.1, 0.5 and 1 wt.% Pt was measured to be in the range of 70–75%, which corresponds to a mean crystallite size (d_{Pt}) of 1.4–1.6 nm. Catalysts of higher metal loading are characterized by lower dispersion and higher crystallite size, i.e., $D = 52\%$ ($d_{Pt} = 2.0$ nm) for 2%Pt/TiO_2 and $D = 34\%$ ($d_{Pt} = 3.1$ nm) for 5%Pt/TiO_2.

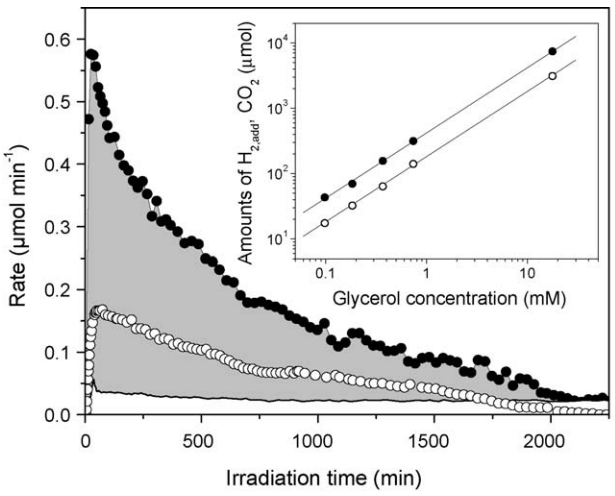

Fig. 1. Rates of H_2 (closed symbols) and CO_2 (open symbols) evolution as functions of time of irradiation obtained from aqueous photocatalyst suspensions in the presence of glycerol. With solid line is shown the hydrogen production curve obtained from pure water. Experimental conditions: photocatalyst: 0.5%Pt/TiO_2 (1.33 g L^{-1}); $C_{glyc} = 0.738$ mM; $T = 40$ °C; solution pH: natural; incident light intensity: 3.79×10^{-7} Einstein s^{-1}. *Inset*: total amounts of $H_{2,add}$ (closed symbols) and CO_2 (open symbols) produced under photo-reforming conditions as functions of initial glycerol concentration in solution. Solid lines correspond to the amounts of products expected from stoichiometry (Eq. (1))

3.2. Effects of the presence of glycerol on photocatalytic performance

Typical results obtained in the absence and in the presence of glycerol (0.738 mM) in solution are shown in Fig. 1, where the rates of H_2 r_{H_2} and CO_2 (r_{CO_2}) evolution are plotted as functions of irradiation time. It is observed that in the presence of glycerol the rate of hydrogen production goes through a maximum of 0.58 μmol min^{-1} at ca. 30 min, which is more than one order of magnitude higher, compared to that obtained from pure water. Prolonged exposure to illumination results in a progressive decrease of (r_{H_2}), which eventually drops to pseudo-steady state values comparable to those obtained in the absence of glycerol. The amount of "additional" hydrogen ($H_{2,add}$) produced due to the presence of glycerol (shadowed area) is equal to 313.7 μmol. Production of H_2 is accompanied by evolution of CO_2 the rate of which goes through a maximum after ca. 75 min and then gradually decreases with time. The total amount of CO_2 produced, estimated by integration of the corresponding rate curve, is equal to 140.6 μmol.

Results of Fig. 1 can be explained by considering that glycerol acts as a sacrificial agent by removing rapidly and irreversibly photogenerated holes, oxidants (e.g., •OH) and/or oxygen produced by cleavage of water [5–7]. This results in suppression of the rates of electron–hole recombination and/or O_2–H_2 back reaction, i.e., processes that decrease the light-to-hydrogen conversion efficiency [9–11]. When the sacrificial agent is fully oxidized to CO_2, photogenerated oxidants can no longer be removed efficiently from the photocatalyst surface and the rate of hydrogen production drops to steady state values comparable to those obtained in the absence of the glycerol. Qualitatively similar results were obtained with the use of variable concentrations of glycerol in the range of 0.1–17.7 mM. In all cases, the amounts of $H_{2,add}$ and CO_2 produced are in very good agreement with those expected from the stoichiometry of the photo-reforming reaction (see inset of Fig. 1), with the molar ratio $H_{2,add}$:CO_2 being practically constant at 7:3.

3.3. Effect of platinum loading on reaction rate

The effect of platinum loading on the reaction rate has been investigated over a set of seven Pt/TiO_2 photocatalysts of variable

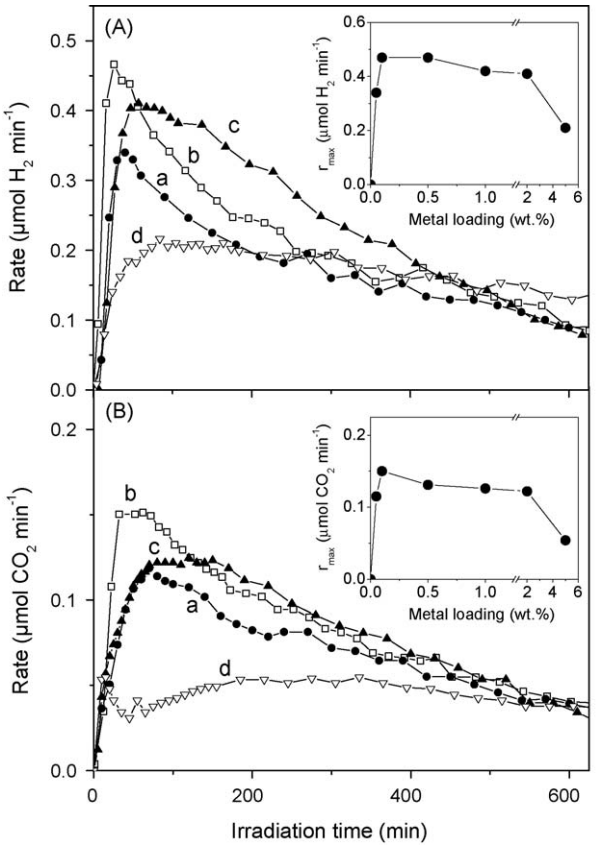

Fig. 2. Rates of (A) H_2 and (B) CO_2 evolution as functions of irradiation time obtained over Pt/TiO_2 photocatalysts of variable metal loading: (a) 0.05, (b) 0.10, (c) 2.0, and (d) 5.0 (wt.% Pt). C_{glyc} = 0.368 mM; other experimental conditions same as in Fig. 1. *Insets*: effect of metal loading on the rate maxima of H_2 and CO_2 evolution

metal content in the range of 0.0–5.0 wt.%. Typical results obtained are shown in Fig. 2, where r_{H_2} (Fig. 2A) and r_{CO_2} (Fig. 2B) are plotted as functions of irradiation time. It should be noted that, under the present experimental conditions, production of hydrogen and CO_2 is negligible over unmetallized TiO_2 indicating that the presence of dispersed Pt nanocrystallites is a prerequisite for the photo-reforming reaction to occur. Dispersion of only 0.05 wt.% Pt on TiO_2 results in evolution of significant amounts of hydrogen (Fig. 2A, trace a), the rate of which goes through a maximum of 0.34 μmol min^{-1} at t = 40 min and then gradually decreases with time of irradiation. Increasing Pt loading to 0.10 wt.% results in an increase of the rate maximum to 0.47 μmol min^{-1} (trace b), which now appears at lower irradiation times (t = 30 min). Further increase of Pt content to 0.5 wt.% does not affect significantly the rate curve (Fig. 5B, vide infra). However, dispersion of even higher amounts of Pt on the photocatalyst surface results in a progressive decrease or r_{max}, which is accompanied by its shift toward higher irradiation times (trace c). This is more pronounced for the high-loaded 5%Pt/TiO_2 photocatalyst (trace d), which is the least active sample of this series. A qualitatively similar effect of Pt content is observed for CO_2 evolution (Fig. 2B). The effect of metal loading on the rate maxima of H_2 and CO_2 production is shown in the insets of Fig. 2. It is observed that optimal photocatalytic performance for the title reaction is obtained for samples loaded with 0.1–0.5 wt.% Pt.

The beneficial effect of dispersed noble metal crystallites on the activity of semiconductor photocatalysts can be attributed to their ability to act as traps of photogenerated electrons thereby enhancing charge separation and retarding electron–hole recombination [12,13]. An essential requirement is that the work function of the metal is higher than that the semiconductor, which is the case for the present system. Dispersed metal crystallites may also behave as classical thermal catalysts and affect the rate of "dark" catalytic reactions and/or selectivity to reaction products. For example, deposition of metal (e.g., Pt) and/or metal oxide (e.g., RuO_2) particles on TiO_2 has been reported to improve kinetics of the water-splitting reaction by decreasing the overpotentials of hydrogen and oxygen evolution, respectively [9,14]. In addition, platinum, which is a good oxidation catalyst, is possible to participate in the title reaction by catalyzing oxidation of glycerol and/or reaction intermediates by photogenerated oxygen.

The presence of an optimum loading value above which metal deposition has a detrimental effect on activity is often observed in photocatalytic reactions [12,13]. For Pt supported on TiO_2, this value is usually lower than 1 wt.% [13], in agreement with results of the present study. Higher Pt loadings generally result in reduced photocatalytic efficiency due to enhanced electron–hole recombination and UV-shielding of the TiO_2 particles by the metal deposits [12]. It is also possible that the observed dependence of the rate on Pt loading is due to variation of the number of active sites located at the metal/support interface, as proposed for photocatalytic reforming of methanol over Pd/TiO_2 photocatalysts [15].

3.4. Effects of operational parameters on photocatalytic performance

3.4.1. Photocatalyst content in suspension

The effect of photocatalyst concentration (C_{cat}) on the apparent reaction rate has been investigated with the use of aqueous glycerol solutions (0.368 mM) containing variable amounts of 0.5%Pt/TiO_2 (0–2.66 g L^{-1}). In the absence of photocatalyst, no measurable amounts of H_2 or CO_2 could be detected in the gas phase. Addition of 0.66 g L^{-1} of photocatalyst results in the production of significant amounts of H_2 and CO_2 (Fig. 3, traces a), the rate curves of which are similar to those obtained for C_{cat} = 1.33 g L^{-1} (Fig. 5B, vide infra). Further increase of photocatalyst content to 1.66 g L^{-1} (traces b) and 2.66 g L^{-1} (traces c) leads to higher initial rates of H_2 and CO_2 evolution but $r_{H_{2,add}}$ and, especially, r_{CO_2} diminish in shorter time periods, compared to those obtained for lower photocatalyst concentrations. This behaviour can be understood by considering that the higher the initial reaction rate the shorter the time period required for completion of the photo-reforming reaction and return of the system to conditions relevant to those corresponding to pure water. This is supported by the fact that the total amounts of additional hydrogen and CO_2 produced are practically the same for all experiments of this series, i.e., 156 ± 4 μmol for $H_{2,add}$ and 63.5 ± 1.5 μmol for CO_2, in agreement with values expected from the stoichiometry of Eq. (1) (154.7 μmol H_2, 66.3 μmol CO_2). This is reasonable because the total amounts of products should not depend on photocatalyst concentration but only on the initial amount of reactant glycerol, which is the same in all cases.

The effect of C_{cat} on the rate maxima of H_2 and CO_2 evolution is shown in the insets of Fig. 3. It is observed that, in both cases, r_{max} initially increases with increase of photocatalyst concentration and then tends to level off. This behaviour, which is typical for reactions occurring in photocatalyst suspensions [16], can be understood by considering that increase of C_{cat} leads to higher surface area of the photocatalyst that is available for absorption of light and adsorption of reactants. However, above a certain limit of photocatalyst concentration, the solution opacity increases and screening effects of particles occur, which mask part of the photosensitive area.

3.4.2. Glycerol concentration

In Fig. 4 are summarized results obtained in our previous [7] and present study with the use of variable glycerol concentrations

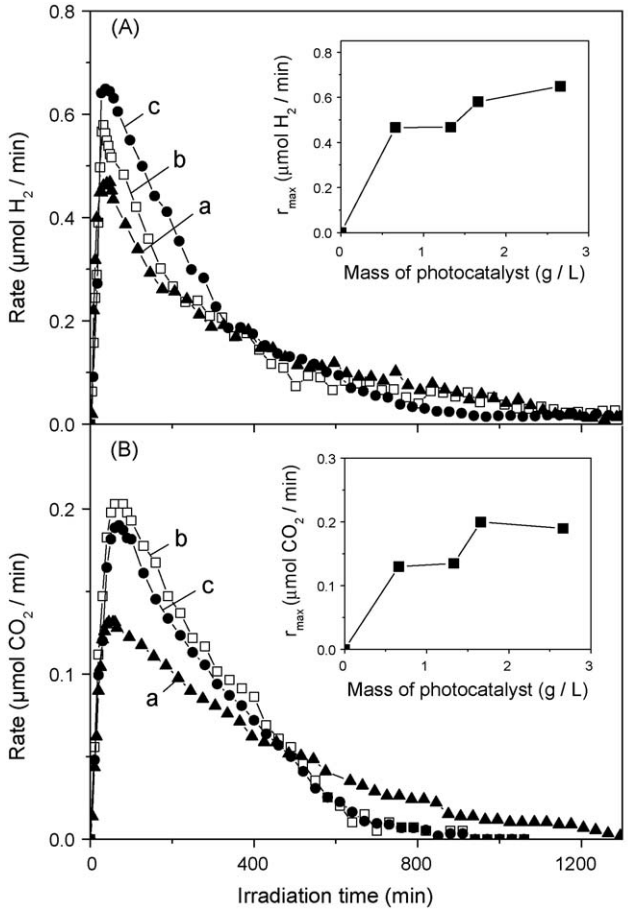

Fig. 3. Rates of (A) H_2 and (B) CO_2 evolution obtained over aqueous glycerol suspensions containing variable amounts of 0.5%Pt/TiO_2 photocatalyst: (a) 0.66 g L^{-1}, (b) 1.66 g L^{-1}, and (c) 2.66 g L^{-1}. C_{glyc} = 0.368 mM; other experimental conditions same as in Fig. 1. *Insets*: effect of photocatalyst content on the rate maxima of H_2 and CO_2 evolution

(C_{glyc}) under otherwise the same experimental conditions. It is observed that increase of C_{glyc} in the range of 0–1086 mM results in a monotonic increase of the rate of H_2 evolution. For relatively low glycerol concentrations ($C_{glyc} < 1$ mM) the rate eventually drops to

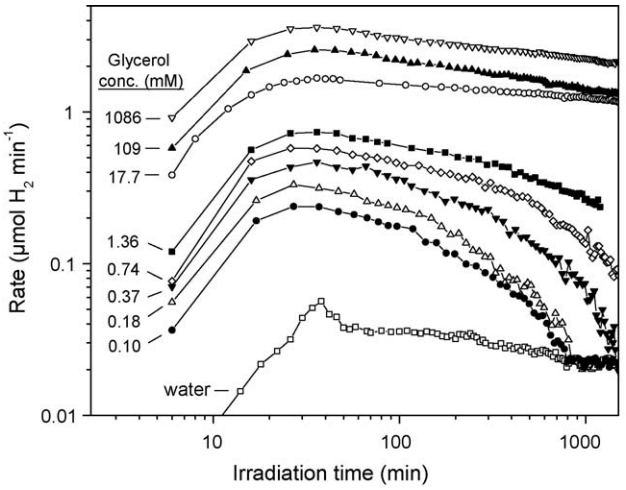

Fig. 4. Rate of hydrogen evolution as function of irradiation time obtained over photocatalyst suspensions containing the indicated glycerol concentrations. Other experimental conditions same as in Fig. 1.

values comparable to those obtained from pure water, indicating that complete conversion of glycerol and reaction intermediates toward H_2 and CO_2 has been achieved. This is verified by the fact that the total amounts of H_2 and CO_2 produced in these experiments are in agreement with those expected from stoichiometry (see inset of Fig. 1). The same is true for C_{glyc} = 17.7 mM, in which case irradiation times longer that 10 days are required to completely reform glycerol (Fig. 7, vide infra). Finally, for much higher glycerol concentrations ($C_{glyc} > 0.1$ M) the rate takes values in the order of 1 μmol min^{-1} for several days, and much longer irradiation periods are required for completely converting glycerol and reaction intermediates to H_2 and CO_2. It is of interest to note that under these conditions r_{H_2} becomes about two orders of magnitude higher, compared to that obtained from pure water.

3.4.3. Solution pH

The rate curves of H_2 and CO_2 evolution obtained over glycerol solutions (0.368 M) of variable pH are summarized in Fig. 5. It is observed that increase of pH from 3 to 8 (Fig. 5A–C) results in a substantial increase of r_{max} (from 0.36 to 0.66 μmol min^{-1} for H_2 and from 0.13 to 0.19 μmol min^{-1} for CO_2) and in completion of

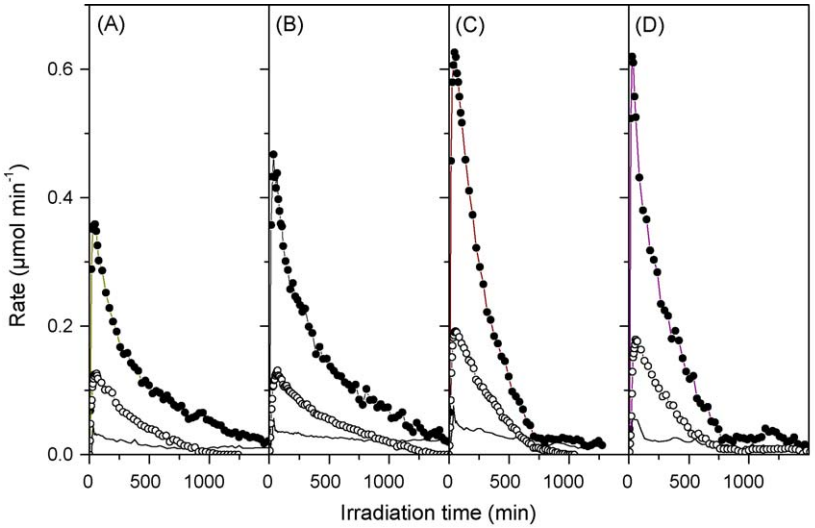

Fig. 5. Effect of solution pH on the rate curves of H_2 (closed symbols) and CO_2 (open symbols) evolution: (A) pH 3, (B) pH 6, (C) pH 8, and (D) pH 10. Hydrogen production curves obtained from pure water are shown with solid lines. C_{glyc} = 0.368 mM; other experimental conditions same as in Fig. 1.

the photo-reforming reaction at shorter time periods. For instance, evolution of $H_{2,add}$ stops at ca. 1500 min at pH 3 (Fig. 5A), compared to ca. 700 min at pH 8 (Fig. 5C). Further increase of solution pH to 10 (Fig. 5D) does not induce significant changes on the rate curves, compared to those obtained at pH 8 (Fig. 5C). Regarding the total amounts of $H_{2,add}$ and CO_2 produced, these are practically the same for experiments conducted at pH 6–10, i.e., 153.9 ± 2.2 μmol min^{-1} for H_2 and 63.7 ± 0.6 μmol min^{-1} for CO_2. In contrast, the total amounts of $H_{2,add}$ (123.0 μmol min^{-1}) and CO_2 (48.0 μmol min^{-1}) evolved at pH 3 are substantially lower than those expected from stoichiometry of Eq. (1) (154.7 μmol H_2, 66.3 μmol CO_2). This indicates that, under these conditions, the photo-reforming reaction is not complete and products other than H_2 and CO_2 are present on the photocatalyst surface and/or in solution at the end of the experiment. Further investigation of this issue is beyond the scope of the present study.

Comparison of results presented in Fig. 5 shows that solution pH affects substantially the rate of H_2 evolution, which is favored at neutral and basic solutions, compared to acidic solutions. Similar results were obtained in our previous study of ethanol photo-reforming [6]. This dependence can be due to several reasons [6,16,17], including the effects of pH on (a) the positions of the valence- and conduction-band levels of the semiconductor with respect to those of the redox couples in solution, (b) the charging behavior of the semiconductor surface, (c) the speciation of substances in solution, and (d) the size of aggregates of photocatalyst particles formed.

3.4.4. Temperature

The effect of solution temperature on photocatalytic performance has been investigated in the range of 40–80 °C and results obtained are presented in Fig. 6. It is observed that increasing temperature from 40 to 60 °C results in an increase of the rate maximum for both hydrogen evolution (from 0.47 to 0.81 μmol min^{-1}) and CO_2 evolution (from 0.13 to 0.23 μmol min^{-1}). This is accompanied by faster completion of the photo-reforming reaction (ca. 800 min at $T = 60$ °C *vs.* 1200 min at $T = 40$ °C). Further increase of temperature to 80 °C does not affect significantly the rate curves.

The observed dependence of the reaction rate on solution temperature cannot be related to light-driven reaction steps, because the band gap energy of the semiconductor is too high for thermal excitation to become significant in the temperature range investigated. Thus, the increased reaction rate at $T = 60$–80 °C, compared to that obtained at $T = 40$ °C, should be due to the effect of temperature on "dark" reaction steps. These include adsorption–desorption equilibria of reactants and products, stabilization of transient intermediates, diffusion of adsorbed species, etc. [16]. It is also possible that temperature affects thermal catalytic reaction steps occurring on the semiconductor surface and/or on the surface of dispersed Pt crystallites, such as oxidation of glycerol and reaction intermediates by photogenerated oxidants adsorbed on the metal surface.

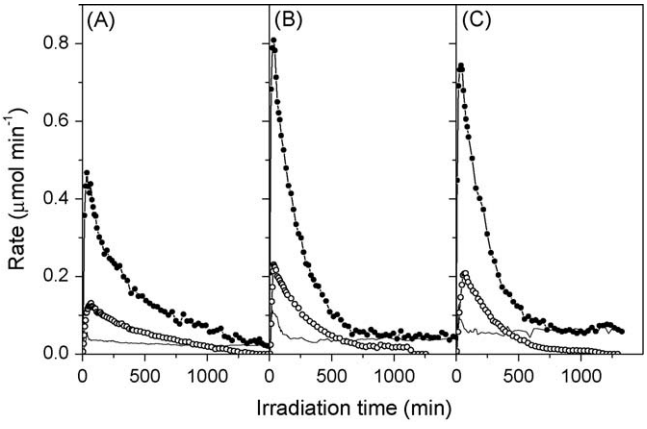

Fig. 6. Effect of temperature on the rates of H_2 (closed symbols) and CO_2 (open symbols) evolution: (A) 40 °C, (B) 60 °C, and (C) 80 °C. Hydrogen production curves obtained from pure water are shown with solid lines. $C_{glyc} = 0.368$ mM; other experimental conditions same as in Fig. 1.

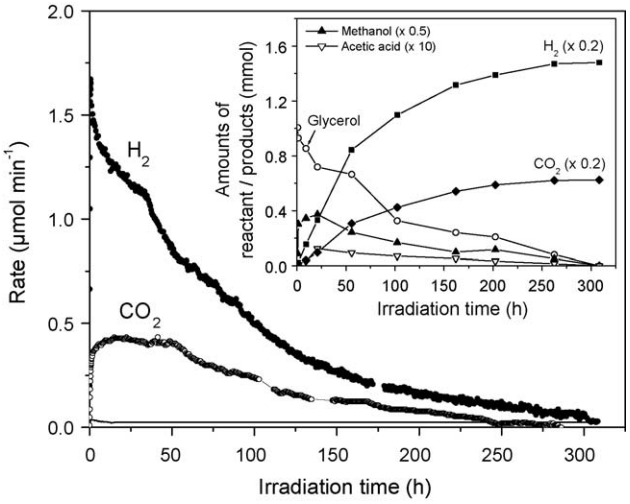

Fig. 7. Rates of H_2 (closed symbols) and CO_2 (open symbols) evolution as functions of irradiation time obtained from aqueous photocatalyst suspensions containing 17.7 mM of glycerol. Other experimental conditions same as in Fig. 1. *Inset*: amounts of reactant, intermediates and final products in the gas and liquid phase as functions of irradiation time

3.5. Identification of reaction intermediates

Formation and fate of reaction intermediates has been investigated with the use of a glycerol solution of sufficiently high concentration (17.7 mM), and results obtained are summarized in Fig. 7. It is observed that under these conditions the irradiation time required for completion of the photo-reforming reaction is about 300 h. Hydrogen and CO_2 were the only products detected in the gas phase. The total amounts of $H_{2,add}$ and CO_2 produced throughout the experiment are in excellent agreement with those predicted from stoichiometry (see inset of Fig. 1). This indicates that reactant glycerol and all reaction intermediates are eventually reformed to CO_2 and H_2.

Identification and quantification of intermediate compounds in the liquid phase has been achieved in separate experiments where the reaction was stopped at the desired irradiation times, the suspension was collected, filtered and stored in sealed vials in a refrigerator for further analysis. Results obtained are shown in the inset of Fig. 7, where the amounts (in mmol) of reactant glycerol and intermediates in solution (methanol, acetic acid) as well as of final products evolved in the gas phase (H_2, CO_2) are plotted as functions of irradiation time. It is observed that the concentration of glycerol decreases progressively with time and disappears after ca. 300 h. The main reaction intermediate is methanol, the amount of which increases rapidly with irradiation time and goes through a maximum at $t = 10$–20 h. This is followed by production of much smaller amounts of acetic acid, which reaches a maximum at ca. $t = 20$ h. Trace amounts of other intermediate compounds detected in the liquid phase could not be identified with certainty and therefore are not discussed further. Prolonged exposure to irradiation results in a progressive decrease of the amounts of all intermediates in solution and, eventually, in their complete conversion to H_2 and CO_2.

Results of the present and previous studies [5–7] clearly show that water acts as an oxidizing agent, via intermediate formation of hydroxyl radicals and other photogenerated oxidants, and that the photo-reforming process occurs via oxidation of the organic compound toward molecules of progressively lower molecular weight and, eventually, CO_2. This results in increased H_2 production rates due to suppression of electron–hole recombination and H_2–O_2 back reaction. Intermediate production of methanol indicates the existence of parallel reaction pathways, which may be similar to those reported for thermal catalytic reforming of oxygenated hydrocarbons in the liquid phase [3,4]. For instance, it has been reported that glycerol aqueous reforming over Pt catalysts at elevated temperatures and high pressure results in the production of a variety of liquid by-products, such as methanol, ethanol, acetone, acetic acid, etc. [7]. It may be suggested that glycerol undergoes dehydrogenation steps on the metal surface to give H_2 and adsorbed intermediates, which is followed by cleavage of C–C bonds and desorption of smaller molecules, such as methanol and acetic acid. These compounds, and also fragments adsorbed on the photocatalyst surface, are subsequently oxidized by photogenerated oxidants toward CO_2. At any case, the overall process may be described as photoreforming of glycerol, since the only final products formed are hydrogen and carbon dioxide.

4. Conclusions

Hydrogen can be produced efficiently by photocatalytic reforming of aqueous solutions of glycerol with the use of Pt/TiO_2 photocatalyst and a solar light-simulating source. Optimal results are obtained for TiO_2 loaded with 0.1–0.5 wt.% Pt, whereas higher metal contents have a detrimental effect on photocatalytic performance. The maximum rate of hydrogen evolution depends strongly on the initial glycerol concentration and increases by about two orders of magnitude with increase of C_{glyc} from 0 to 1 M. The reaction rate is higher at neutral and basic solutions, and increases with increasing temperature from 40 to 60–80 °C. Glycerol is a low (or negative) cost by-product of biodiesel manufacturing and therefore the photo-reforming process may provide a viable method of renewable hydrogen production.

Acknowledgments

This work is co-financed by E.U.-European Social Fund (80%) and the Greek Ministry of Development-GSRT (20%) under the PENED 2003 Program (contract 03ED607).

References

[1] J.A. Turner, Science 305 (2004) 972.
[2] F. Ma, M.A. Hanna, Bioresour. Technol. 70 (1999) 1.
[3] R.R. Davda, J.W. Shabaker, G.W. Huber, R.D. Cortright, J.A. Dumesic, Appl. Catal. B 56 (2005) 171.
[4] N. Luo, X. Fu, F. Cao, T. Xiao, P.P. Edwards, Fuel 87 (2008) 3483.
[5] A. Patsoura, D.I. Kondarides, X.E. Verykios, Appl. Catal. B 64 (2006) 171.
[6] A. Patsoura, D.I. Kondarides, X.E. Verykios, Catal. Today 124 (2007) 94.
[7] D.I. Kondarides, V.M. Daskalaki, A. Patsoura, X.E. Verykios, Catal. Lett. 122 (2008) 26.
[8] P. Panagiotopoulou, D.I. Kondarides, J. Catal. 225 (2004) 327.
[9] A.J. Bard, J. Phys. Chem. 86 (1982) 172.
[10] K. Hashimoto, T. Kawai, T. Sakata, J. Phys. Chem. 88 (1984) 4083.
[11] T. Sakata, J. Photochem. 29 (1985) 205.
[12] O. Carp, C.L. Huisman, A. Reller, Prog. Solid State Chem. 32 (2004) 33.
[13] A.L. Linsebigler, G. Lu, J.T. Yates Jr., Chem. Rev. 95 (1995) 735.
[14] D. Duonghong, E. Borgarello, M. Grätzel, J. Am. Chem. Soc. 103 (1981) 4685.
[15] A. Dickinson, D. James, N. Perkins, T. Cassidy, M. Bowker, J. Mol. Catal. A 146 (1999) 211.
[16] J.-M. Herrmann, Top. Catal. 34 (2005) 49.
[17] C. Kormann, D.W. Bahnemann, M.R. Hoffmann, Environ. Sci. Technol. 25 (1991) 494.